Hydrogen passivation effect in nitrogen-doped ZnO thin films

Xiaonan Li, Brian Keyes, Sally Asher, S. B. Zhang, Su-Huai Wei, and Timothy J. Coutts
National Renewable Energy Laboratory, Golden, Colorado 80401

Sukit Limpijumnong
School of Physics, Institute of Science, Suranaree University of Technology, Nakhon Ratchasima 30000, Thailand

Chris G. Van de Walle
Materials Department, University of California at Santa Barbara, Santa Barbara, California 93106

(Received 13 September 2004; accepted 14 February 2005; published online 17 March 2005)

The role of hydrogen in nitrogen-doped ZnO thin films was studied by Fourier transform infrared (FTIR) absorption and modeled by first-principles calculations to understand the difficulty of doping ZnO *p*-type with nitrogen. Nitrogen-doped ZnO films were fabricated by low-pressure metal-organic chemical vapor deposition (MOCVD). High levels of nitrogen incorporation were observed, but the acceptor concentrations remained low. Theoretical analysis suggests there is a high probability that N_O^- and H^+ charged defects combine to form the neutral defect complexes, thereby compensating the nitrogen-related acceptors. Calculated values of the vibrational frequencies of the related infrared modes agree well with the measured spectra. Thus, we believe the difficulty of achieving *p*-type doping in MOCVD-grown ZnO films is due, at least partially, to inadvertent passivation by hydrogen. © *2005 American Institute of Physics*. [DOI: 10.1063/1.1886256]

ZnO is a wide-band-gap (~3.3 eV) semiconductor that has been used extensively in optoelectronic devices such as solar cells and surface acoustic wave devices.[1–3] However, it has always been used as an *n*-type semiconductor. It is relatively straightforward to make *n*-type ZnO, but it is very difficult to make *p*-type material.[4,5] There is considerable commercial appeal in using ZnO to replace III–V semiconductors for various applications. In recent years, much effort has been devoted to fabricating *p*-ZnO, and there is now substantial evidence that several groups have achieved this goal.[6–12] However, *p*-type material often has poor quality; it is characterized by low hole concentration and mobility, and tends to revert to *n*-type behavior over the course of months at room temperature. The origin of these problems is far from being fully understood, and the results obtained from different groups appear to be rather inconsistent.

To date, the hole concentration achieved in *p*-type ZnO has been limited to 10^{18}–10^{19} cm^{-3}, with a resistivity of 10^{-2}–10^{-3} Ω cm, using group V dopants.[7,8,11,13] However, such low resistivity has not been achieved in ZnO grown by metal-organic chemical vapor deposition (MOCVD) with nitrogen doping. In MOCVD samples, typical carrier concentrations have been 10^{14}–10^{18} cm^{-3}, although the concentration of nitrogen has been as high as 10^{21} cm^{-3}.[9,14] The reasons for the low carrier concentration are unclear. It could be due to several reasons: (1) only a small fraction of nitrogen can substitute for oxygen (N_O) and become an acceptor. (2) N_O acceptors have a large ionization energy. (3) The N_O acceptors are compensated or passivated. Previous theoretical study suggested that the ionization energy of the isolated N_O acceptor is large (~0.4 eV).[15] However, other reports have assigned the 0.16 eV level observed experimentally to the N_O related acceptor level.[16,17] The exact position of the N_O level is, therefore, still under debate.

Hydrogen, which is present in the Zn growth precursor, could easily be incorporated in the ZnO film during its growth. Hydrogen is known to be amphoteric in most semiconductors, but is always a donor in ZnO and, hence, can passivate acceptors such as N_O.[18,19] Here, using experimental measurements and theoretical calculations, we argue that hydrogen and nitrogen interact strongly to form a neutral defect complex, thereby reducing the maximum achievable hole concentration.

Nitrogen-doped ZnO thin films were grown using low-pressure MOCVD with diethylzinc [DEZn, $(C_2H_5)_2Zn$] and dilute NO gas (2 wt. % NO/Ar) were used as precursors and nitroge as the carrier gas. The deposition temperature was 400 °C. Undoped films were made with DEZn and O_2 gas. Corning 1737 glass substrates were used for most characterizations. For FTIR measurements, special-shaped Si substrates were used to enhance the signal intensity.

The hydrogen and nitrogen concentrations were analyzed using secondary-ion mass spectroscopy (SIMS, Cameca IMS 5f) and x-ray photoelectron spectroscopy (XPS, Physical Electronics Model 5600), respectively. The electrical properties were studied using Hall measurements (Bio-Rad Model HL5500). The N–H bond signatures were studied using FTIR transmittance measurements at room temperature.[20]

The preliminary results from SIMS profiles on these MOCVD-formed ZnO films indicate that the hydrogen level is several orders higher than the background level and varies with the DEZn flow rate. This suggests that the hydrogen in the films might originate from DEZn. The systematic analysis of the nitrogen concentration with fabrication variables was reported previously.[21] The typical nitrogen concentration in our ZnO:N samples is about 1–3 at %, corresponding to 0.87–2.60×10^{21} cm^{-3}.

The electronic properties of the film studied in this work are clearly divided into two groups. The undoped ZnO films deposited at 400 °C are *n*-type with an electron concentration in the range of 10^{16}–10^{18} cm^{-3} and resistivity of about 1 Ω cm. With nitrogen doping, the films become weakly *p*-type. The film resistivity is on the order of 10^2 Ω cm or

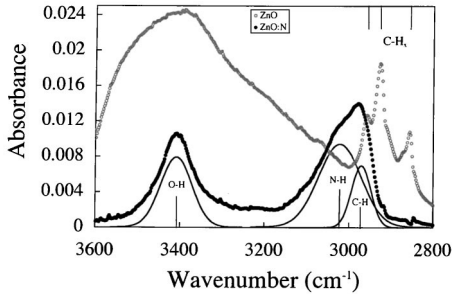

FIG. 1. FTIR absorbance spectra of undoped (gray dots) and *N*-doped ZnO films (black dots) obtained in the wave number range of 2800–3600 cm^{-1}. The curve fitting for the *N*-doped sample provides 3 Gaussian peaks (solid lines) located at 3410, 3020, and 2970 cm^{-1}. The peak positions of the $C-H_x$ LVM found from the undoped ZnO film are indicated on the top of the plot.

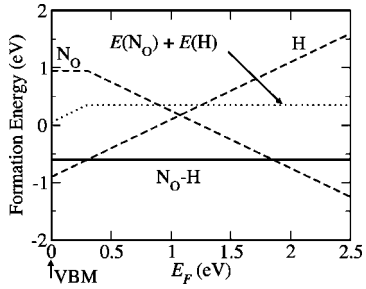

FIG. 2. Calculated formation energy of an interstitial hydrogen, a N_O (dashed lines) and a N_O-H complex (solid line) as a function of electron Fermi energy, referencing to the top of the valence band maximum of ZnO. The dotted line shows the sum of the formation energies of an isolated interstitial hydrogen and an isolated N_O. The Zn-rich condition, N_2 phase precipitation limits (for nitrogen chemical potential), and H_2 phase precipitation limits (for hydrogen chemical potential) were used in the calculations. The slopes of the curves reflect the charge states of the defects.

higher. The carrier concentration is in the range of $10^{13}-10^{15}$ cm^{-3}. Compared to the nitrogen concentration in the order of 10^{21} cm^{-3}, the achieved carrier concentration is low.

The FTIR absorbance spectra of undoped and *N*-doped films in the wave number range 2500–4000 cm^{-1} were studied. Several important local stretch modes, involving hydrogen bonded to carbon, nitrogen, and oxygen, are located in this spectral region. For undoped ZnO film, the IR spectrum (gray dots in Fig. 1) is characterized by $C-H_x$ absorption peaks around 2900 cm^{-1} and a broad asymmetrical band around 3400 cm^{-1}, most likely due to an O–H bond. With incorporation of nitrogen (black dots in Fig. 1), the broad asymmetrical band around 3400 cm^{-1} becomes a narrower and more symmetrical peak at 3410 cm^{-1}, which could be due to a surface mode of an O–H bond.[22] Furthermore, the peaks around 2900 cm^{-1} mostly disappeared. Instead, a new peak formed at 3007 cm^{-1}, which can be fit by individual Gaussian peaks at 3020 and 2970 cm^{-1}. The peak at 2970 cm^{-1} is possibly due to the remaining $C-H_x$ bonds, and the peak at 3020 cm^{-1} is a new peak. We also performed FTIR measurements at a temperature of about 11 K in an attempt to resolve closely spaced peaks. For these measurements, the sample was measured in the straight-through configuration, because a low temperature ATR holder was not available. Unfortunately, the films were very thin, the signal to noise ratio suffered accordingly and an increase in resolution was not found. Nevertheless, we observed peaks at similar frequencies as in the room temperature case.

To understand the changes in the FTIR spectrum and the interaction between nitrogen and hydrogen in ZnO, we have calculated the formation energies of an interstitial hydrogen atom, a nitrogen acceptor N_O, and a N_O-H complex. We performed first-principles calculations based on density functional theory with local density approximation (LDA) and ultrasoft pseudopotential as implemented in the VASP codes.[23] The definition of formation energy of a defect from first-principles calculations has been described in various publications.[24,25] The theoretical calculation of possible hydrogen-related local vibration frequency is performed following the approach in Ref. 26, which properly includes the anharmonic part of the vibrations.

To estimate the error in frequency caused by the computational approach (e.g., pseudopotentials and LDA), we calculated the symmetric stretch-mode frequency of a free ammonia (NH_3) molecule and compared it with experimental data. Our calculated result of 3194 cm^{-1} is about 143 cm^{-1} smaller than the experimental value of 3337 cm^{-1}.[27] We assume that this underestimation is systematic and that our calculated frequency for the N–H stretch modes in ZnO are consistently lower by this amount.

Interstitial hydrogen is predicted to act exclusively as a donor in ZnO, i.e., always in the 1^+ charge state.[18] Hydrogen prefers four low-energy sites surrounding an O atom in the wurtzite structure.[28] Our calculations, as well as those of Ref. 22, showed the bond-center ($BC_\parallel$) site, parallel to the *c*-axis, to be the site with the lowest energy. Hydrogen at the other three sites has slightly higher energy (to within about 0.2 eV). Only the lowest formation energy of this defect is used for the plot in Fig. 2.

Figure 2 shows the calculated formation energy of an interstitial H, a substitutional N, (N_O), and the complex between the two (N_O-H) as a function of the Fermi energy. The Fermi energy is referenced to the top of ZnO valence band maximum (VBM). Over most of the Fermi energy range, the N_O is stable in a $1-$ charge-state, thus is attracted to the positively charged H donor. The formation energy of the neutral N_O-H complex (solid line) is lower in energy than the sum of the formation energies of the individual defects (dotted line) by 0.95 eV, that is, the neutral complex has a binding energy of 0.95 eV. An important consequence of this, for the interpretation of FTIR data, is that, in the presence of N_O acceptors, hydrogen atoms will tend to passivate the acceptors (i.e., forming N–H bonds with N_O acceptors) instead of existing as interstitial donor H (i.e., forming O–H bonds with host O atoms).

The microscopic structure of N_O in the (1^-) charge-state is illustrated in Fig. 3(a). Hydrogen can occupy four high-symmetry sites surrounding the nitrogen atom, two BC and two antibonds (AB_N) [Fig. 3(b)]. We have examined all four sites and identified the $AB_{N_\perp}$ configuration to be the site with the lowest formation energy. The relative formation energy, local stretch-mode vibration frequency, and calculated N_O-H bond distance for all four configurations are listed in Table I. Again, only the formation energy of the lowest energy configuration (in this case, $AB_{N_\perp}$) is used in the plot of Fig. 2. From Table I, we can see that both AB_N configurations have similar N_O-H stretch-mode frequencies, with an average value of 2927 cm^{-1}. Both BC configurations have similar N_O-H stretch-mode frequencies with an average

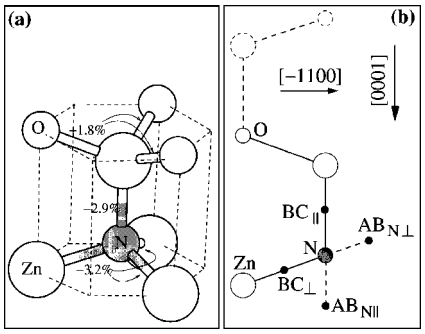

FIG. 3. (a) Atomic structure of the N_O acceptor in ZnO in the $(1-)$ charge-state and (b) possible hydrogen sites surrounding the N_O acceptor in the (11–20) plane of wurtzite ZnO. The large white spheres are the Zn, the small white spheres are the O, and the small shaded spheres are the N atoms. In (a), the bond lengths are given in terms of the percentage differences from bulk ZnO bond. In (b), small solid circles represent the possible sites for hydrogen.

value of 3319 cm^{-1}, i.e., larger than the AB_N modes. To compare the calculated frequencies with those observed by FTIR, we applied the systematic error of 143 cm^{-1} to the calculated N–H vibration frequencies, thereby increasing the calculated values to 3070 and 3462 cm^{-1} for the AB_N and BC modes, respectively. The 3070 cm^{-1} AB_N mode is close to the observed local vibrational mode (LVM) at 3020 cm^{-1} in the *N*-doped sample, whereas the 3462 cm^{-1} LVM falls into the region that overlaps with O–H LVM. However, the calculation also reveals that the AB_N configurations are energetically more stable than the BC by about 0.2–0.3 eV. With this energy difference, the possibility of forming the BC configuration is negligible. From the analysis above, we are therefore confident in assigning the observed absorption band at 3020 cm^{-1} to N_O-H in the AB_N configuration. In addition, the partially disappeared absorption bands around 3400 cm^{-1} and 2900 cm^{-1} caused by nitrogen doping could be explained by the reduced quantity of hydrogen that bonds with oxygen and carbon due to the existing of N_O-H bonds.

An additional test calculation using slightly different computational details (using pseudopotential as implemented in the FHI98 codes, similar to the calculations details used in Ref. 26, instead of ultrasoft pseudopotentials) yield results in qualitative agreement with VASP calculations. For examples, the $AB_{N_\perp}$ configuration is also found to be the site with the lowest formation energy (the other sites are slightly higher by about 0.2 eV) with the vibrational frequency of 3117 cm^{-1}, i.e., agrees to the VASP calculations to within 50 cm^{-1}.

In summary, we have performed composition, electronic, and FTIR characterization on MOCVD-grown ZnO thin films, with and without nitrogen doping. Hydrogen was detected by SIMS analysis, which suggested the existence of unintentional hydrogen doping of the films. Hall analysis indicated weak *p*-type behavior, with hole concentrations in the range $10^{13}-10^{15}$ cm^{-3}. The absorption bands in the O–H and C–H LVM spectral region partially disappeared and a new IR absorption peak at 3020 cm^{-1} was introduced as a result of the nitrogen doping.

With first-principles calculations, we have assigned the IR spectral features at 3020 cm^{-1} to N_O-H LVM at AB_N configuration. There is a strong tendency for hydrogen to compensate nitrogen and form a neutral N_O-H defect complex, thus we believe this could be an important cause of the low hole concentration in MOCVD-grown ZnO:N films.

TABLE I. Calculated relative formation energy, N–H bond distance, and vibration frequency for N_O-H defect complex in four lowest-energy configurations in wurtzite ZnO. ω^0 is the harmonic component of the vibrational frequency, $\Delta\omega$ is the anharmonic contribution, and ω is the total frequency: $\omega=\omega^0+\Delta\omega$.

Site	ΔE (eV)	d_{N-H} (A)	ω^0 (cm^{-1})	$\Delta\omega$ (cm^{-1})	ω (cm^{-1})
$AB_{N_\perp}$	0.00	1.050	3144	−232	2912
$AB_{N_\parallel}$	0.08	1.047	3173	−232	2941
$BC_\perp$	0.32	1.027	3395	−88	3307
$BC_\parallel$	0.18	1.029	3478	−147	3331

The authors would like to thank James Keane for sample preparation, Craig Perkins for nitrogen concentration analysis, and Matthew Young for SIMS characterization. This work was supported by the U.S. Department of Energy under Contract No. DE-AC36-99GO10337. The work in Thailand was supported by the Thailand Research Fund under Contract No. BRG4680003.

[1] A. E. Delahoy and M. Cherny, Mater. Res. Soc. Symp. Proc. **426**, 467 (1996).
[2] J. Hu and R. G. Gordon, Sol. Cells **30**, 437 (1991).
[3] C. R. Goria, N. W. Emanetoglu, S. Liang, W. E. Mayo, Y. Lu, M. Wraback, and H. Shen, J. Appl. Phys. **85**, 2595 (1999).
[4] S. J. Pearton, D. P. Norton, K. Ip, Y. W. Heo, and T. Steiner, J. Vac. Sci. Technol. B **22**, 932 (2004).
[5] D. C. Look, Mater. Sci. Eng., B **B80**, 383 (2001).
[6] K. Minegishi, Y. Koiwai, Y. Kikuchi, K. Yano, M. Kasuga, and A. Shimizu, Jpn. J. Appl. Phys., Part 1 **36**, L1453 (1997).
[7] M. Joseph, H. Tabata, and T. Kawai, Jpn. J. Appl. Phys., Part 1 **38**, L1205 (1999).
[8] Y. R. Ryu, S. Zhu, D. C. Look, J. M. Wrobel, H. M. Jeong, and H. W. White, J. Cryst. Growth **216**, 330 (2000).
[9] X. Li, Y. Yan, T. A. Gessert, C. Dehart, C. L. Perkins, D. Young, and T. J. Coutts, Electrochem. Solid-State Lett. **6**, C56 (2003).
[10] X.-L. Guo, H. Tabata, and T. Kawai, J. Cryst. Growth **223**, 135 (2001).
[11] T. Aoki, Y. Shimizu, A. Miyake, A. Nakamura, Y. Nakanishi, and Y. Hatanaka, Phys. Status Solidi B **229**, 911 (2002).
[12] A. B. M. A. Ashrafi, I. Suemune, H. Kumano, and S. Tanaka, Jpn. J. Appl. Phys., Part 1 **41**, L1281 (2002).
[13] Kyoung-Kook Kim, Hyun-sik Kim, Dae-Kue Hwang, Jae-Hong Lim, and Seong-Ju Park, Appl. Phys. Lett. **83**, 63 (2003).
[14] B. S. Li, Y. C. Liu, Z. Z. Zhi, D. Z. Shen, Y. M. Lu, J. Y. Zhang, X. W. Fan, R. X. Mu, and D. O. Henderson, J. Mater. Res. **18**, 8 (2003).
[15] C. H. Park, S. B. Zhang, and Su-Huai Wei, Phys. Rev. B **66**, 073202 (2002).
[16] B. K. Meyer, H. Alves, D. M. Hofmann, W. Kriegseis, D. Forster, F. Bertram, J. Chresten, A. Hoffmann, M. Strabburg, M. Dworzak, U. Haboeck, and A. V. Rodina, Phys. Status Solidi B **241**, 231 (2004).
[17] A. Zeuner, H. Alves, D. M. Hofmann, B. K. Meyer, A. Hoffmann, U. Haboeck, M. Strassburg, and M. Dworzak, Phys. Status Solidi B **234**, R7 (2002).
[18] C. G. Van de Walle, Phys. Status Solidi B **229**, 221 (2002).
[19] A. Kamata, H. Mitsuhashi, and H. Fujita, Appl. Phys. Lett. **63**, 3354 (2003).
[20] B. M. Keyes, L. M. Gedvilas, X. Li, and T. J. Coutts (to be published).
[21] X. Li, Y. Yan, T. A. Gessert, C. L. Perkins, D. Young, C. Dehart, and T. J. Coutts, J. Vac. Sci. Technol. A **21**, 1342 (2003).
[22] E. V. Lavrov, J. Weber, F. Borrnert, C. G. Van de Walle, and R. Helbig, Phys. Rev. B **66**, 165205 (2002).
[23] G. Kresse and J. Furthmüller, Comput. Mater. Sci. **6**, 15 (1996).
[24] S. B. Zhang and J. E. Northrup, Phys. Rev. Lett. **67**, 2339 (1991).
[25] S. Limpijumnong, S. B. Zhang, S.-H. Wei, and C. H. Park, Phys. Rev. Lett. **92**, 155504 (2004).
[26] S. Limpijumnong, J. E. Northrup, and C. G. Van de Walle, Phys. Rev. B **68**, 075206 (2003).
[27] S. Limpijumnong, in *Hydrogen in Semiconductors*, edited by N. H. Nickel, M. D. McCluskey, and S. B. Zhang, MRS Symp. Proc. No. 813 (Materials Research Society, Pittsburgh, 2004), H 3.6.
[28] C. G. Van de Walle, Phys. Rev. Lett. **85**, 1012 (2000).